Search for gamma-ray spectral modulations in Galactic pulsars as a result of photon-ALPs mixing.

Jhilik Majumdar
Collaboration: Francesca Calore and Dieter Horns.
JCAP 04(2018)048 (ArXiv: 1801.08813)

June 18, 2018

Institute for Experimentalphysics, University of Hamburg

PATRAS 2018, DESY, Hamburg.

Detection of Axions/ALPs with photons

Axion decay to photons

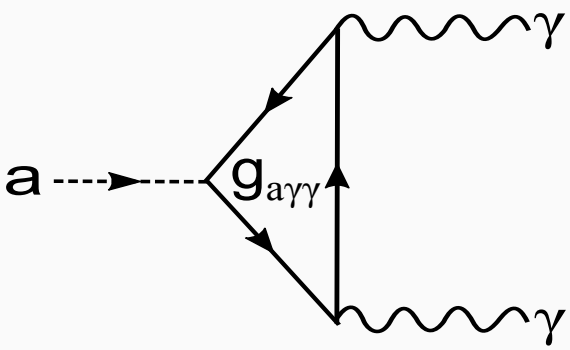

Primakoff process

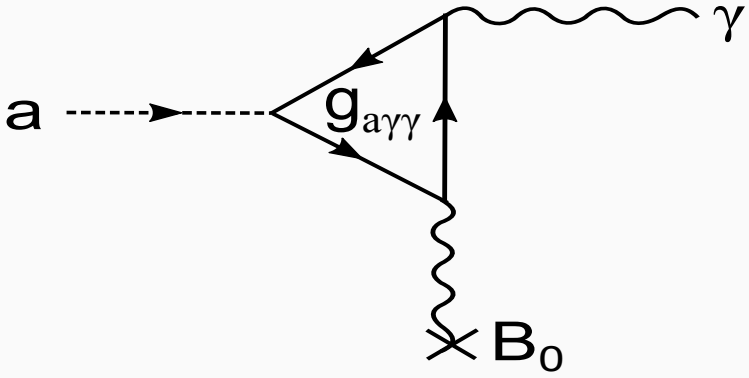

Axion/ALPs have the property:

Oscillate into photons or vice-versa at the presence of magnetic field via Primakoff process.

$$\mathcal{L} \supset -\frac{1}{4} g_{a\gamma\gamma} F_{\mu\nu} \tilde{F}^{\mu\nu} a = g_{a\gamma\gamma}\, \vec{E} \cdot \vec{B}\, a\,, \tag{1}$$

[Raffelt and Stodolsky 88, Sikivie 83.]

Photon-ALP mixing matrix

$$\mathcal{M}_0' = \begin{pmatrix} \Delta_{\parallel} & \Delta_{a\gamma} \\ \Delta_{a\gamma} & \Delta_a \end{pmatrix}. \tag{2}$$

The matrix is made diagonal by a rotation about an angle,

$$\frac{1}{2}\tan 2\theta = \frac{\Delta_{\mathrm{a}\gamma}}{\Delta_{\parallel} - \Delta_{\mathrm{a}}} \tag{3}$$

In analogy to neutrino oscillations, the conversion probability for axion to photon,

$$\mathrm{P}_{\mathrm{a}\to\gamma} = \sin^2(2\theta)\sin^2(\frac{1}{2}\Delta_{\mathrm{osc}}\mathrm{l}), \tag{4}$$

$$\Delta_{osc} = 2\Delta_{a\gamma}\sqrt{1+\left(\frac{E_c}{E}\right)^2} \tag{5}$$

$$sin(2\theta) = \frac{2\Delta_{a\gamma}}{\Delta_{osc}} = \frac{1}{\sqrt{1+\left(\frac{E_c}{E}\right)^2}} \tag{6}$$

$$\Delta_{\parallel} = \Delta_{pl} + 2\Delta_{QED} \tag{7}$$

$$\Delta_{pl} = -\omega_{pl}/2E \tag{8}$$

$$\Delta_a = -m_a^2/2E \tag{9}$$

$$\Delta_{a\gamma} = 1/2 g_{a\gamma\gamma} B_{\perp} \tag{10}$$

Photon-ALPs conversion in magnetic field.

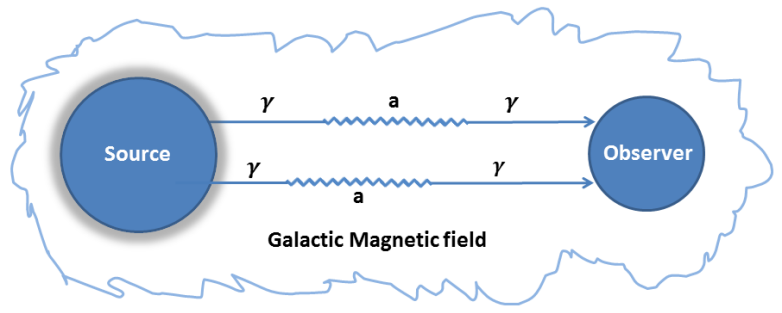

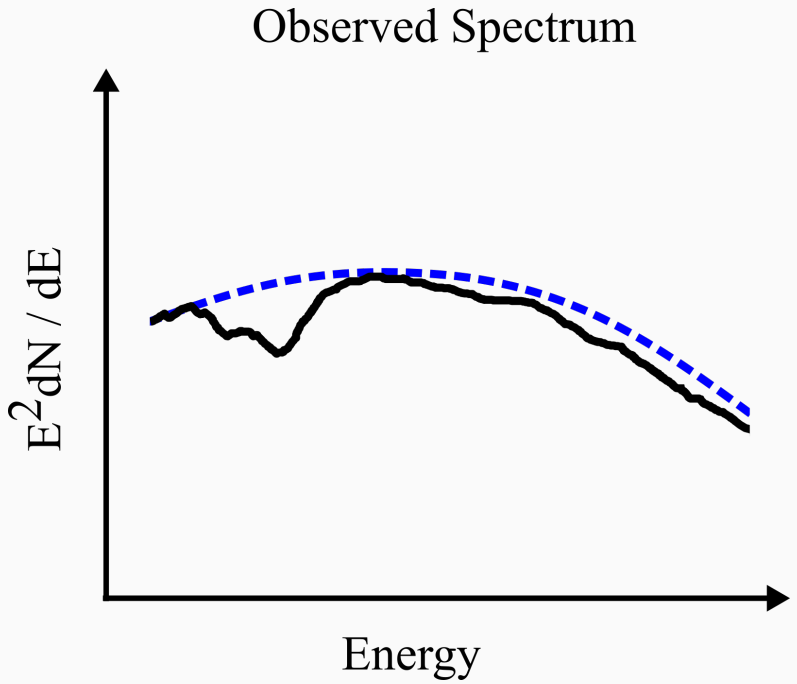

The photon-ALPs oscillation is efficient at energies larger than a critical photon energy E_c ,

$$E_c = \frac{|m_a^2 - \omega_{Pl}^2|}{4\Delta_{a\gamma}} \simeq 2.5\ \mathrm{GeV} \frac{|m_a^2 - \omega_{Pl}^2|}{1\,\mathrm{neV}} \left(\frac{B_\perp}{\mu\mathrm{G}}\right)^{-1} \left(\frac{g_{a\gamma\gamma}}{10^{-11}\ \mathrm{GeV}^{-1}}\right)^{-1}, \quad (11)$$

Photon-ALPs conversion in magnetic field.

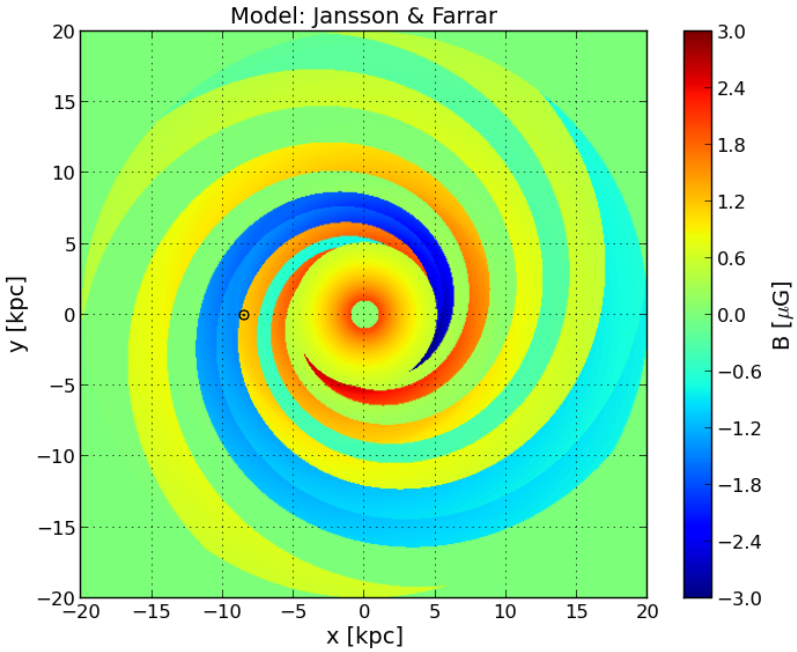

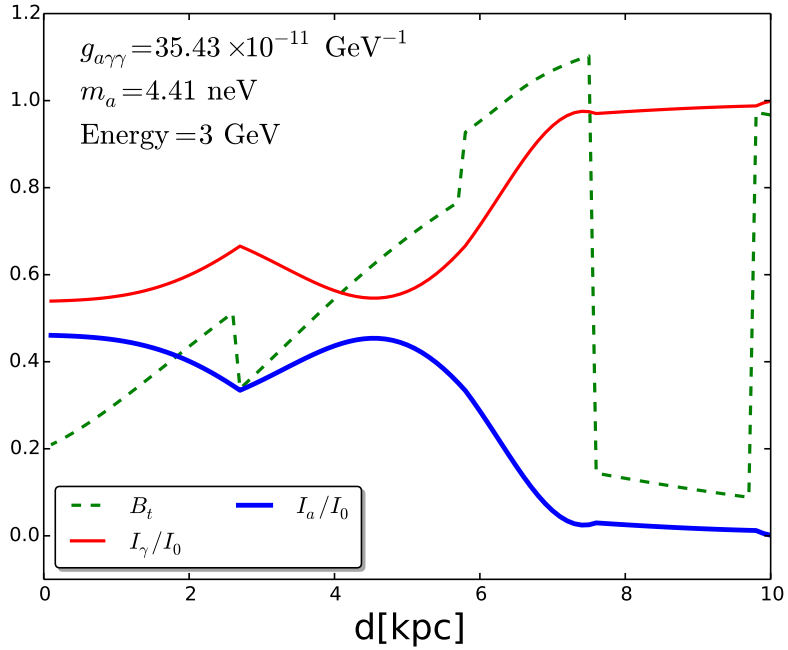

Photon (red thin line) and ALPs (blue thick line) intensity along the line of sight towards PSR J2021+3651. The green dashed line marks the transversal magnetic field.

- **We investigate for the photon-ALPs oscillation features in the disappearance channel in IGMF .**

Detecting gamma rays by Fermi LAT

- Gamma ray space telescope.
- Field of view : 20% of sky at a time.
- Effective area: $1m^2$.
- Energy range from about 100 MeV to more than 500 GeV.
- Period: 1.6 hours(on orbit).
- Energy resolution: $< 5\%$ above 300 MeV.

Fermi Large Area Telescope [Image Credit: NASA/Fermi LAT Collaboration]

Source selection

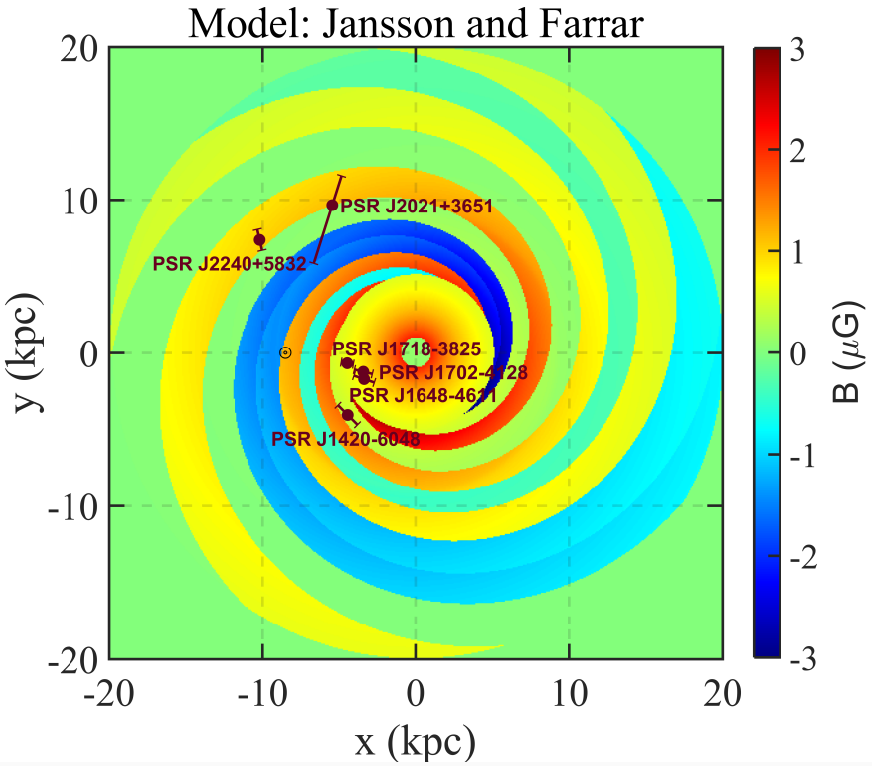

Source positions in the plane of Galactic magnetic field (Jansson & Farrar model; Jansson et al. 2012).]

Source selection criterion:

- Bright galactic source.
- Located at large pitch angle.
- Photons coming from the sources are crossing the spiral arms along the line of sight.

Pulsar list:

1. J2021+3651
2. J1420-6048
3. J2240+5831
4. J1648-4611
5. J1718-3825
6. J1702-4182

Fermi-LAT data analysis:

- 9 years of Fermi LAT data Pass 8 data [Ackermann et al. 2014].
- ENRICO binned likelihood optimization technique has been performed(Sanchez & Deil, 2013).
- Energy region: 100 MeV to 300 GeV.
- Energy bins: 25.
- ROI : 15°.
- Diffused Galactic emission are kept fixed.
- Pulsar spectrum is modelled by a power law with sub exponential cutoff:

$$\frac{dN}{dE} = N_0 \left(\frac{E}{E_0}\right)^{-\Gamma_1} exp\left[\left(-\frac{E}{E_{cut}}\right)^{-\Gamma_2}\right] \tag{12}$$

- We perform a fit to the data, minimizing the χ^2 function.
- Energy dispersion matrix (D_{kk_p}) derived for all the EDISP event types together.

Fermi-LAT data analysis

- Approach: data driven method to calculate systematic uncertainties.
- Source used : Vela (dist - $0.294^{+0.076}_{-0.050}$ kpc).

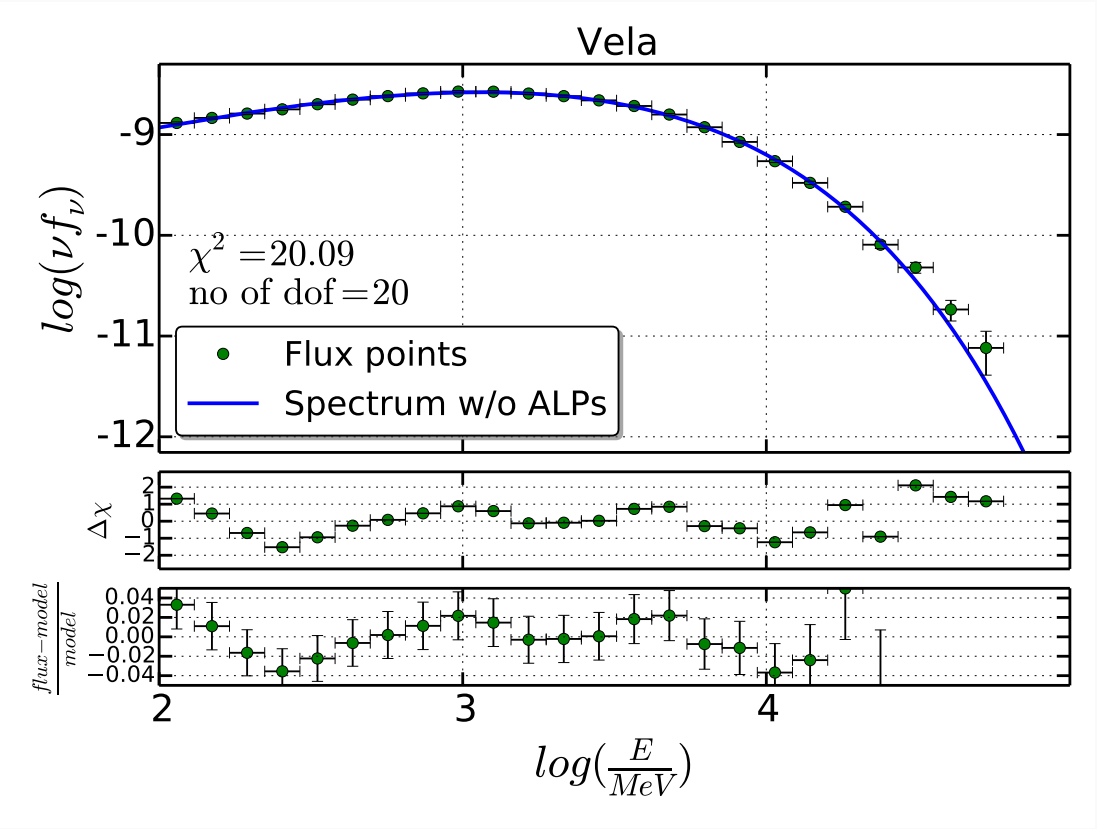

$$N_0 = 105 \times \mathrm{MeV}^{-1}\mathrm{cm}^{-2}\mathrm{s}^{-1}$$
$$\Gamma_1 = 1.27$$
$$E_{cut} = 0.654\mathrm{GeV}$$
$$\Gamma_2 = 0.541$$

- For P8R2 SOURCE V6 event class, systematic uncertainties in effective collection area are derived to be about 2.4 %.

Fermi-LAT data analysis

- signature of photon-ALPs oscillations, including the effect of oscillations in the predicted spectra:

$$\left(\frac{dN}{dE}\right)_{\text{w/o ALPs}} = D_{kk_p} \cdot \left(\frac{dN}{dE}\right)_{\text{intrinsic}}, \tag{13}$$

and

$$\left(\frac{dN}{dE}\right)_{\text{w ALPs}} = D_{kk_p} \cdot (1 - P_{\gamma\to a}(E, g_{a\gamma\gamma}, m_a, d)) \cdot \left(\frac{dN}{dE}\right)_{\text{intrinsic}}, \tag{14}$$

- Photon survival probability calculation: electron density model in the interstellar medium and Galactic magnetic field included.

[M. Meyer et al. PRD 87 (2013),
R. Jansson et al. 2012.]

Hypotheses

Tested hypotheses, i.e. H_0, H_1 and H_2.

Hypotheses	Assumptions
H_0	No ALPs fit following eq. 13.
H_1	Modification according to eq. 14, $\mathrm{g}_{\mathrm{a}\gamma\gamma}$, m_a left free for each source.
H_2	Modification according to eq. 14, $\mathrm{g}_{\mathrm{a}\gamma\gamma}$, m_a globally fit.

- Spectral fitting including H_0 : N_0, Γ and E_{cut}.
- Spectral fitting including H_1 : N_0, Γ, E_{cut}, m_{a} and $\mathrm{g}_{\mathrm{a}\gamma\gamma}$.
- As mass and coupling is unified: Spectral fitting including H_2.

Pulsar spectra

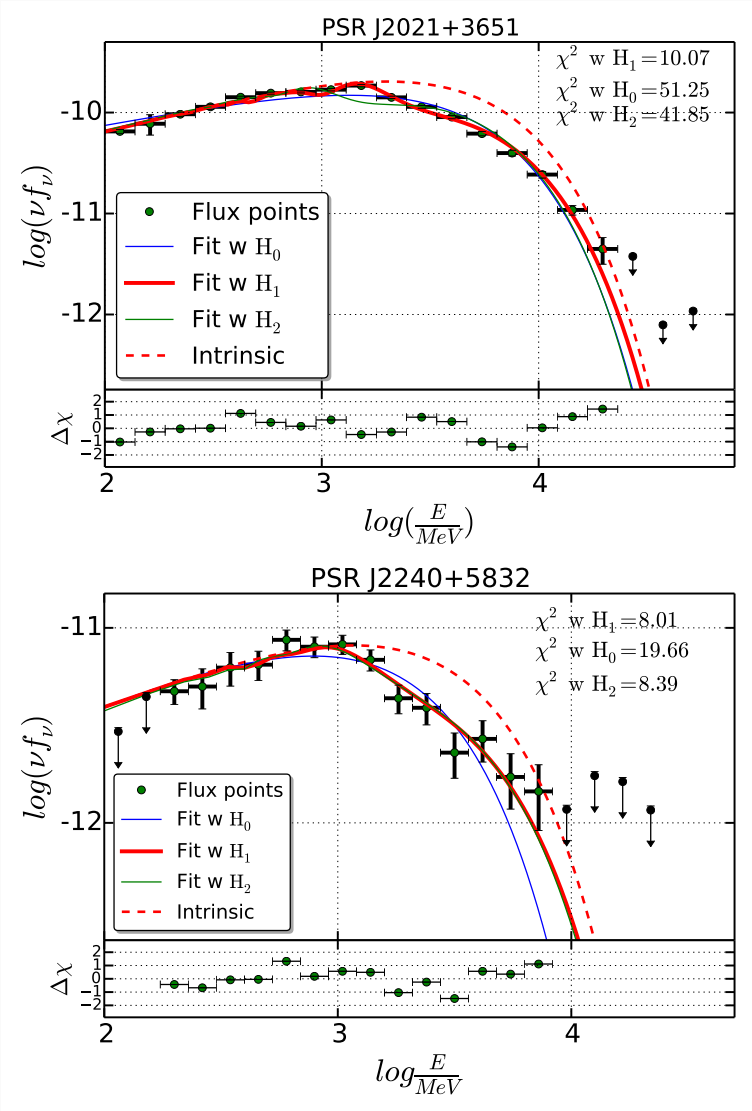

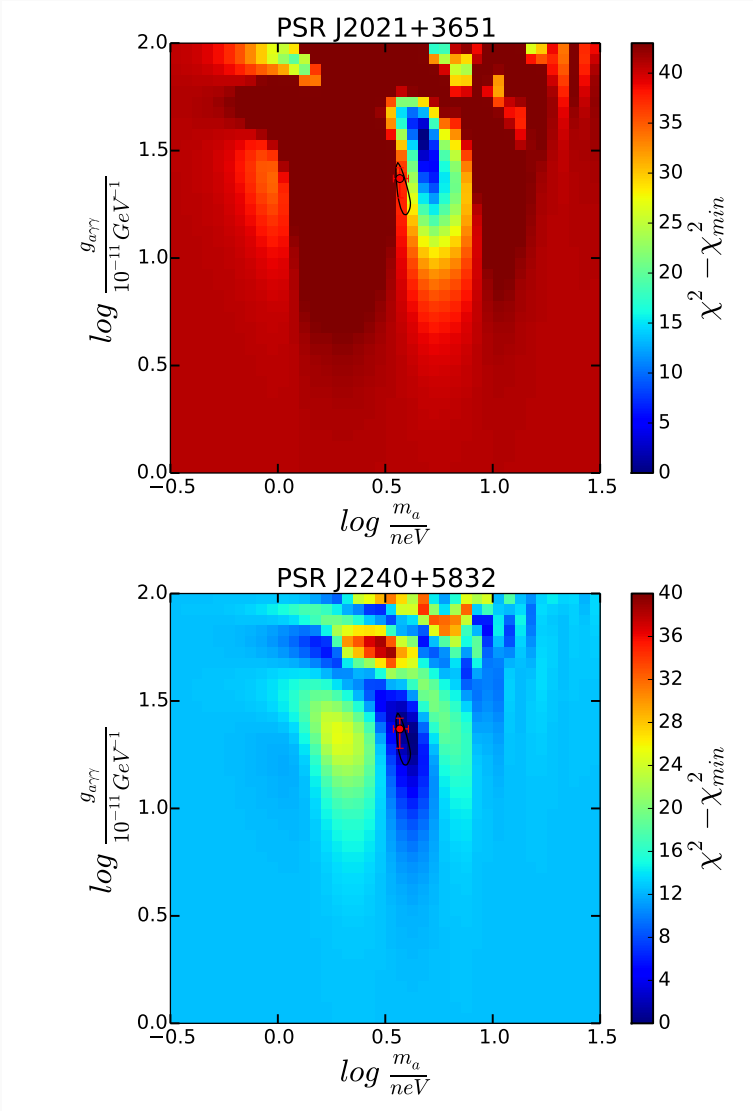

Left panel: **Best-fit model of the spectrum of Pulsar candidates.**

Right panel: **The χ^2 scan as a function of $g_{a\gamma\gamma}$ and m_a.**

Combined Photon-ALPs coupling and ALPs mass sensitivity

Best fit parameter values.

- ALPs mass (m_a) = $(3.6^{+0.5_{\text{stat.}}}_{-0.2_{\text{stat.}}} \pm 0.2_{\text{syst.}})$ neV.
- Photon-ALPs coupling constant $(g_{a\gamma\gamma}) = (2.3^{+0.3_{\text{stat.}}}_{-0.4_{\text{stat.}}} \pm 0.4_{\text{syst.}}) \times 10^{-10}$ GeV^{-1}.

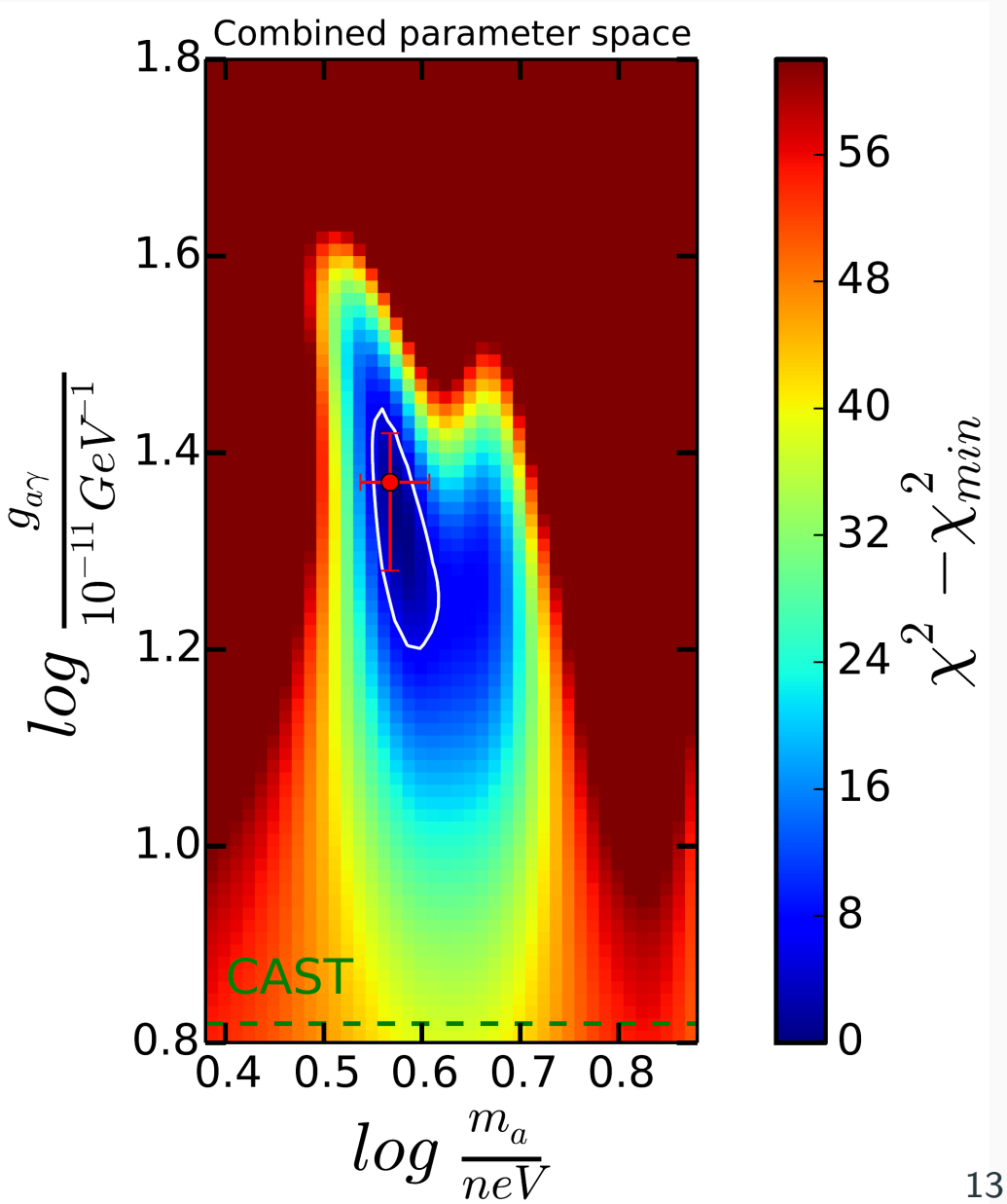

Significance level

Pulsar name	$\chi^2(dof)$ H_0	$\chi^2(dof)$ H_1	Significance (H_1/H_0)	$\chi^2(dof)$ H_2
J1420-6048	31.10(15)	21.27(13)	1.38 σ	22.46(15)
J1648-4611	47.15(14)	21.37(12)	2.38 σ	41.61(14)
J1702-4128	12.70(8)	3.57(6)	2.01 σ	8.54(8)
J1718-3825	53.57(15)	25.61(13)	2.40 σ	29.52(15)
J2021+3651	51.25(14)	10.07(12)	3.86 σ	41.85(14)
J2240+5832	19.66(11)	8.01(9)	2.11 σ	8.39(11)
Combined	215.42(77)	89.9(65)	5.52 σ	152.37(75)

A comparison of the χ^2 values obtained for the three hypotheses.

- Individual spectral fit: H_1 is quite significant.
- Combined spectral fit: H_2/H_0 although deteriorates, holds a significance level 4.6 σ.

Comparison with other parameter space

Limits on ALPs parameter space in the $(m_a, g_{a\gamma\gamma})$ plane.

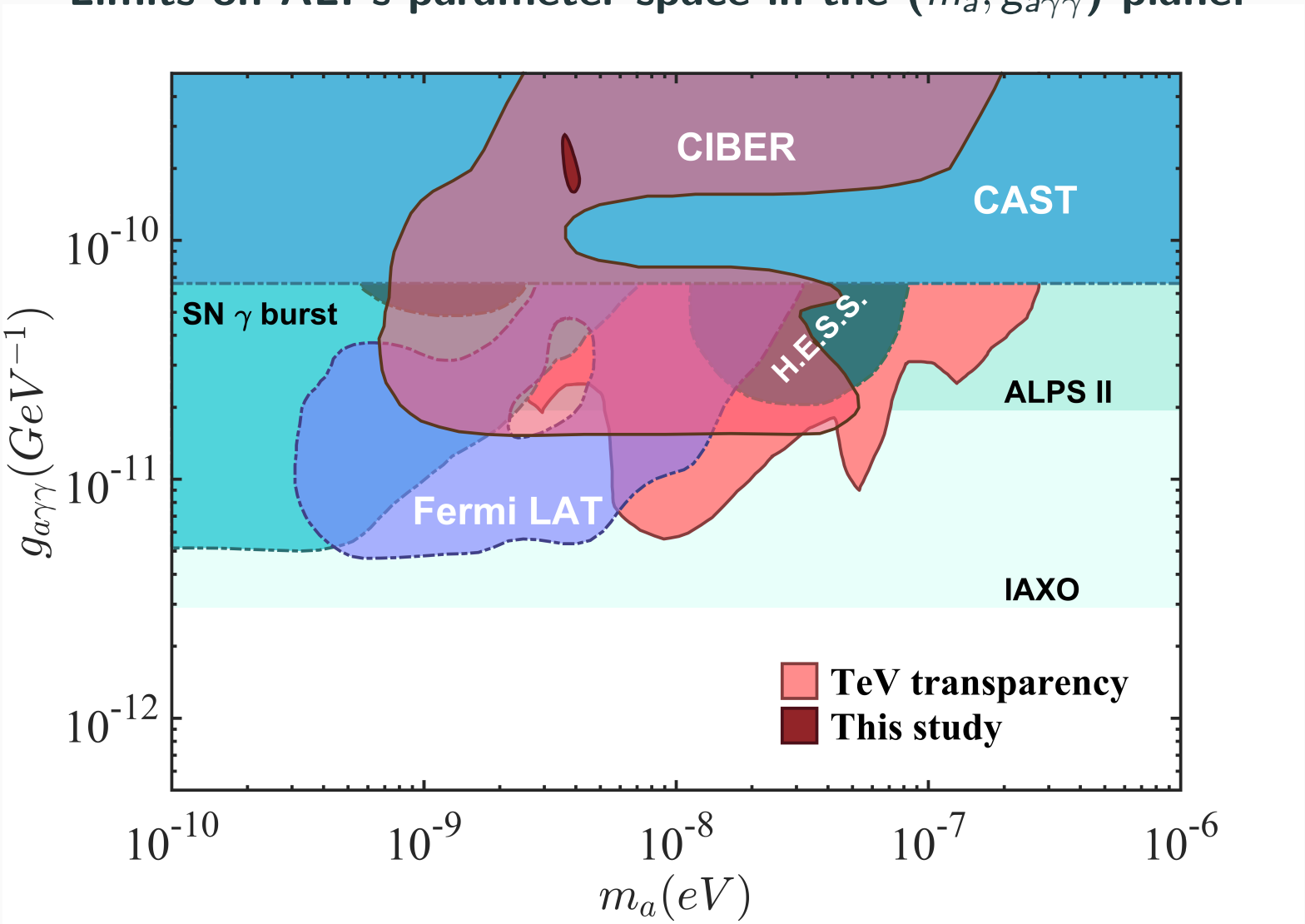

J Majumdar, F Calore and D Horns; JCAP04(2018)048.

Further studies with non-Galactic plane pulsars

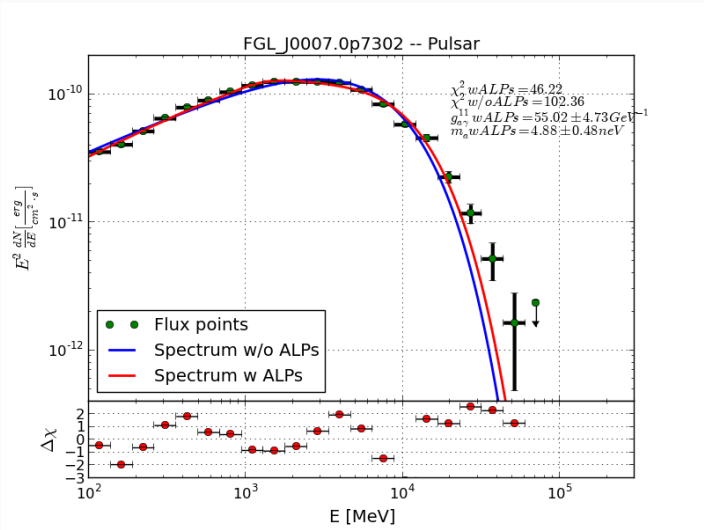

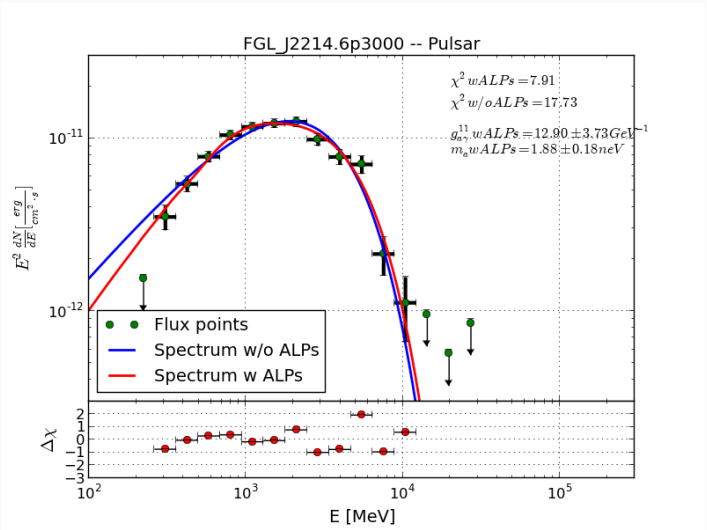

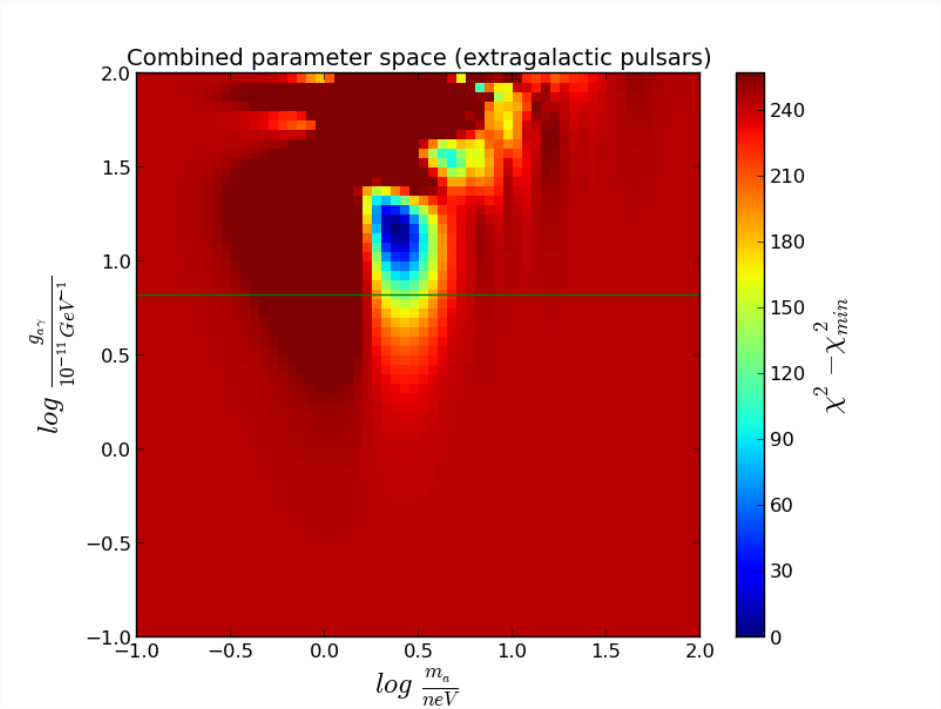

Pulsar name
J0007.0+7302
J0030.4+0451
J0357.9+3206
J0614.1-3329
J1231.2-1411
J1311.8-3430
J1836.2+5925
J2055.8+2539
J2124.7-3358
J2214.6+3000
J2229.7-0833
J2241.6-5237
J2302.7+4443

Further studies with non-Galactic plane pulsars

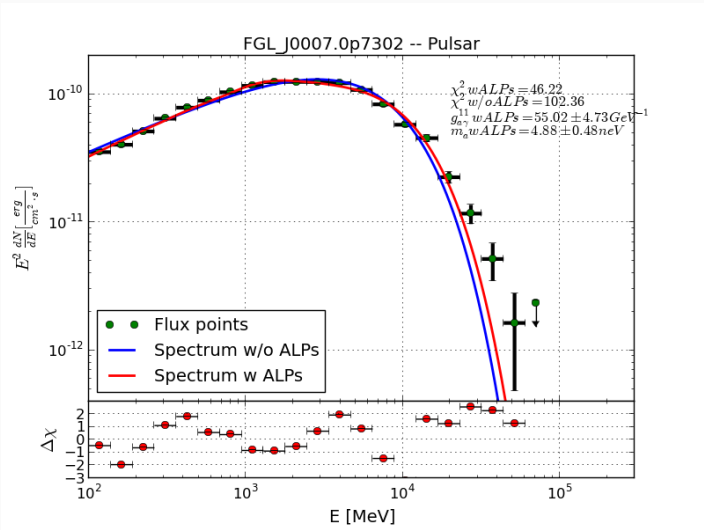

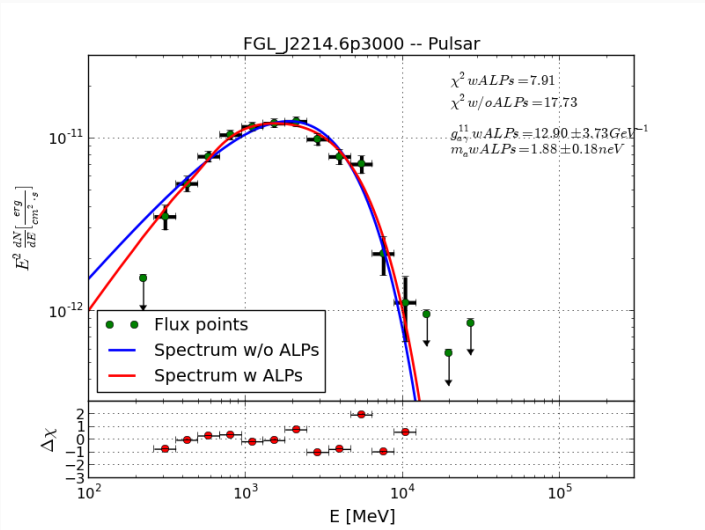

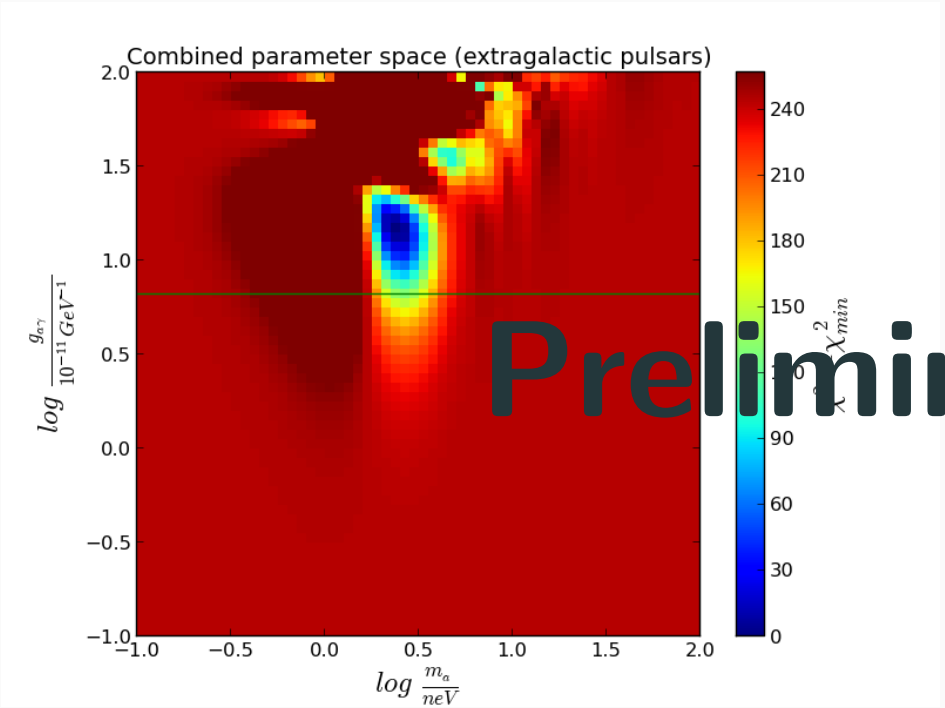

Preliminary

Pulsar name
J0007.0+7302
J0030.4+0451
J0357.9+3206
J0614.1-3329
J1231.2-1411
J1311.8-3430
J1836.2+5925
J2055.8+2539
J2124.7-3358
J2214.6+3000
J2229.7-0833
J2241.6-5237
J2302.7+4443

Summary

- Indications for ALPs in case of Fermi LAT data of **Galactic pulsar candidate**.
- Photon-ALPs mixing is non-linear in the spiral arms and in the large scale field of the inner Galaxy.
- Favourite ALPs mass : $(3.54^{+0.5_{\mathrm{stat.}}}_{-0.2_{\mathrm{stat.}}} \pm 0.2_{\mathrm{syst.}})$ neV.
- Favourite Photon-ALPs coupling constant: $(2.3^{+0.3_{\mathrm{stat.}}}_{-0.4_{\mathrm{stat.}}} \pm 0.4_{\mathrm{syst.}}) \times 10^{-10} GeV^{-1}$.
- Combined significance: 4.6 σ.
- The resulting mixing parameters are quite magnetic field model dependent.
- Similar effects observed with Pshirkov magnetic field model.

Thank you for listening. Any questions?

Backup slides

Axion

- QCD vacuum CP-violating term:

$$L \sim \frac{\alpha_s}{8\pi}\theta G^a_{\mu\nu}\tilde{G}^{a,\mu\nu} \qquad (15)$$

- Observable effect: electric dipole moment of the neutron, strength depends on θ, expected of order unity.
- Solution: introduce new symmetry U(1) PQ, spontaneously broken at scale $\mathrm{f_a}$.

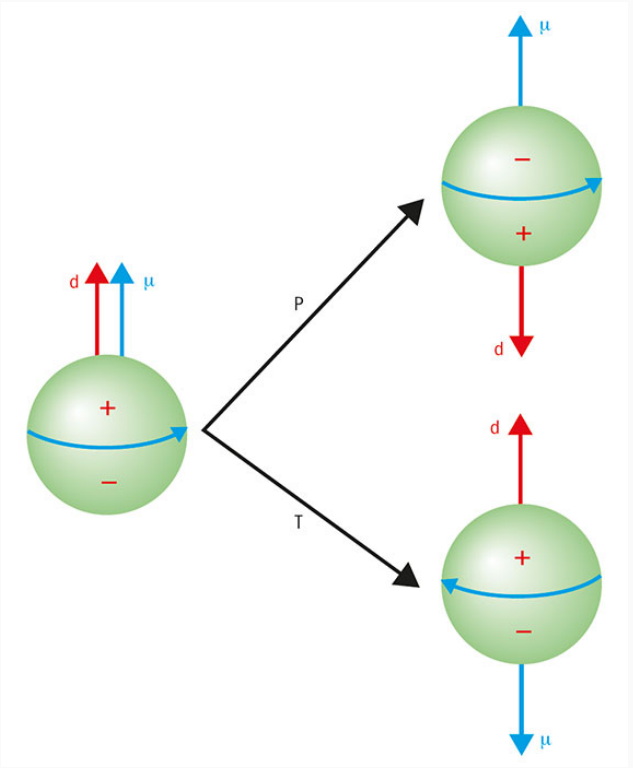

Gamma ray sky with Fermi LAT

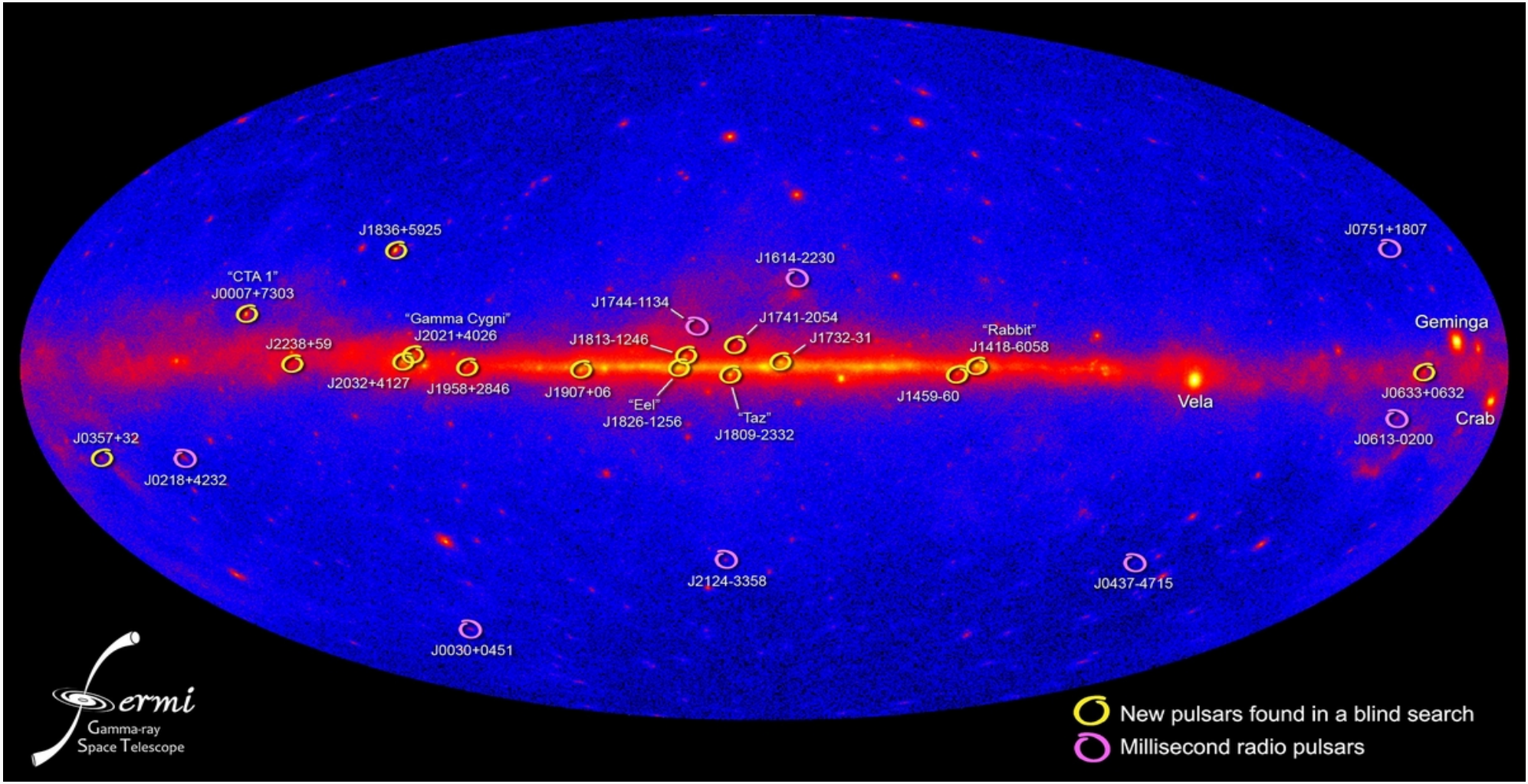

No of γ-ray Pulsars: 160, PWN: 9.

[3FGL catalog, Fermi LAT Collaboration 2015.]

Pulsar spectra

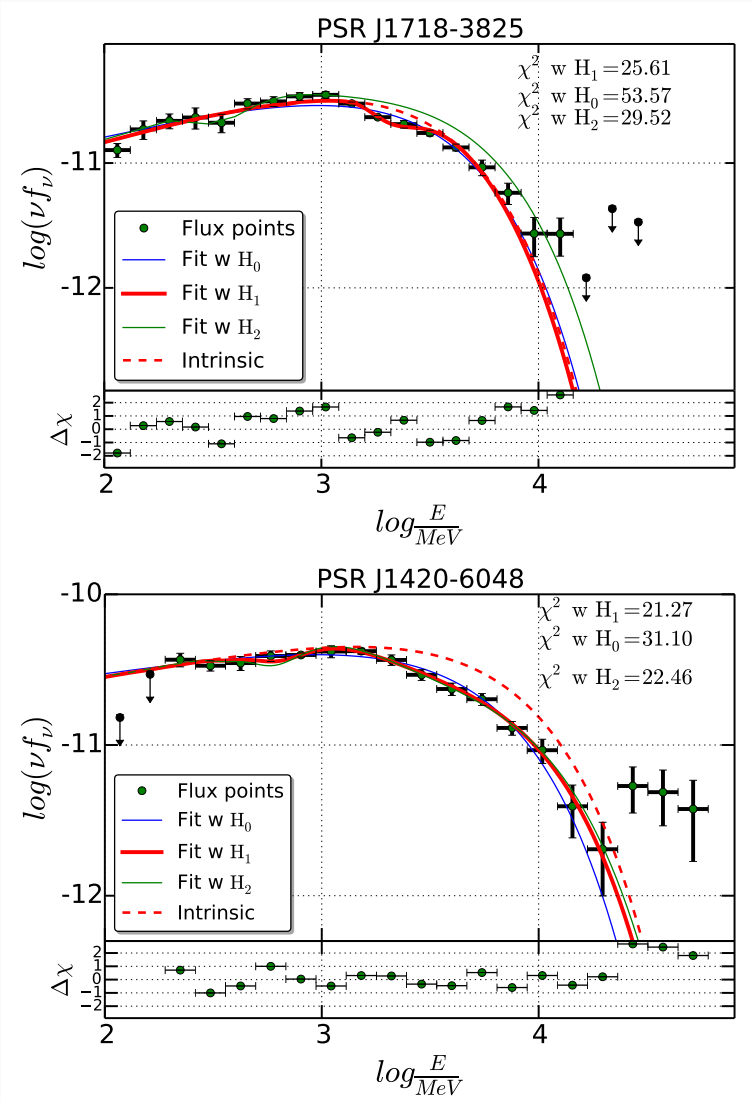

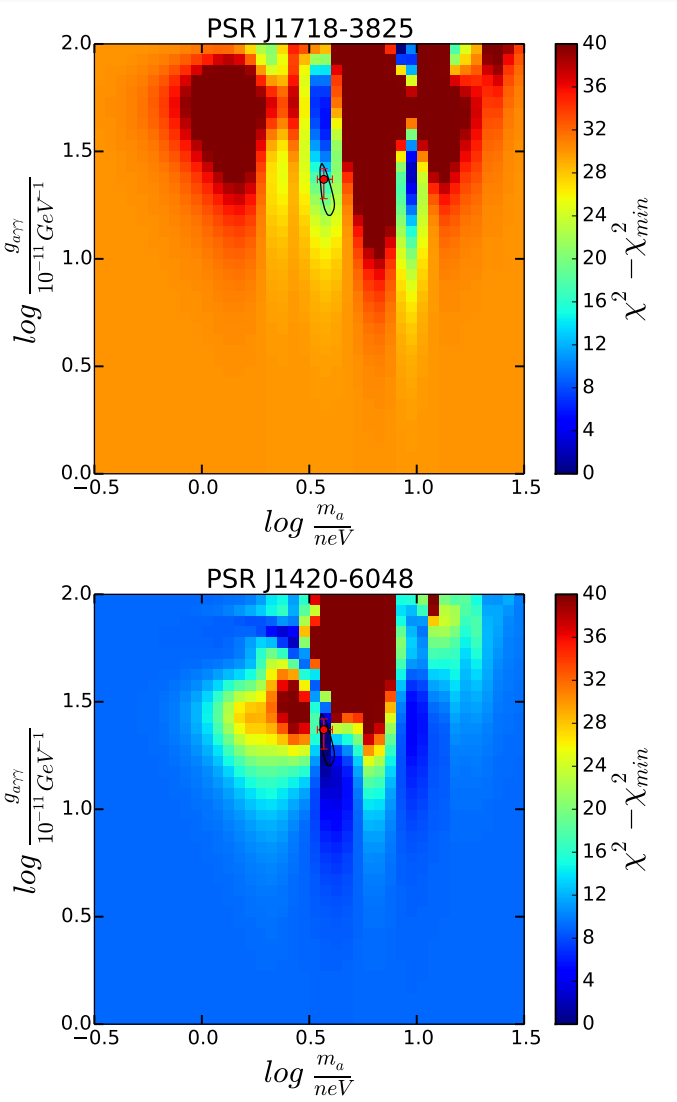

Left panel: **Best-fit model of the spectrum of Pulsar candidates.**

Right panel: **The χ^2 scan as a function of $g_{a\gamma\gamma}$ and m_a.**

Pulsar spectra

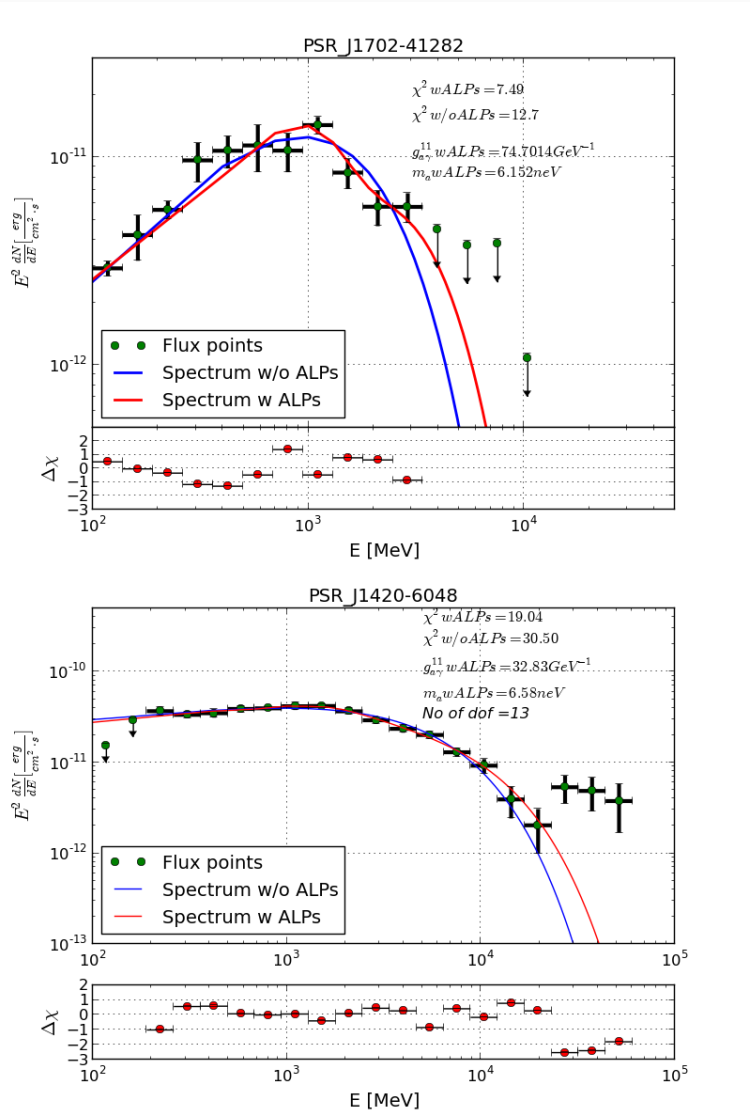

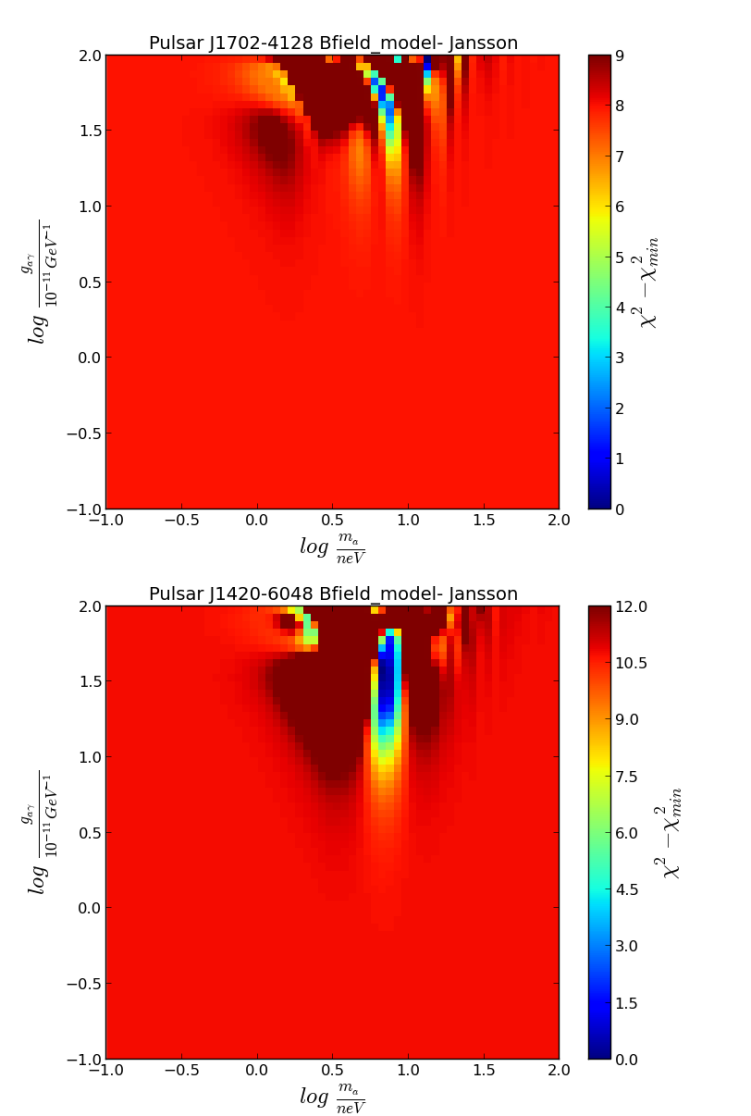

Figure 2: Best-fit model of the spectrum of Pulsar candidates. Right panel: The χ^2 scan as function of photon-ALPs coupling and ALPs mass.

back up slides

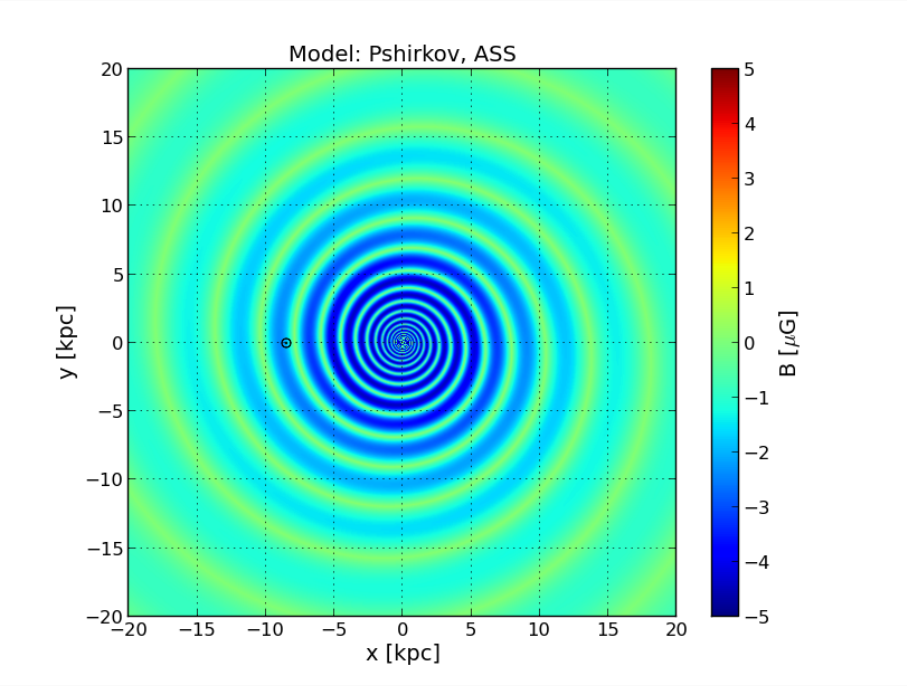

Figure 3: Bfield model: Pshirkov ASS model

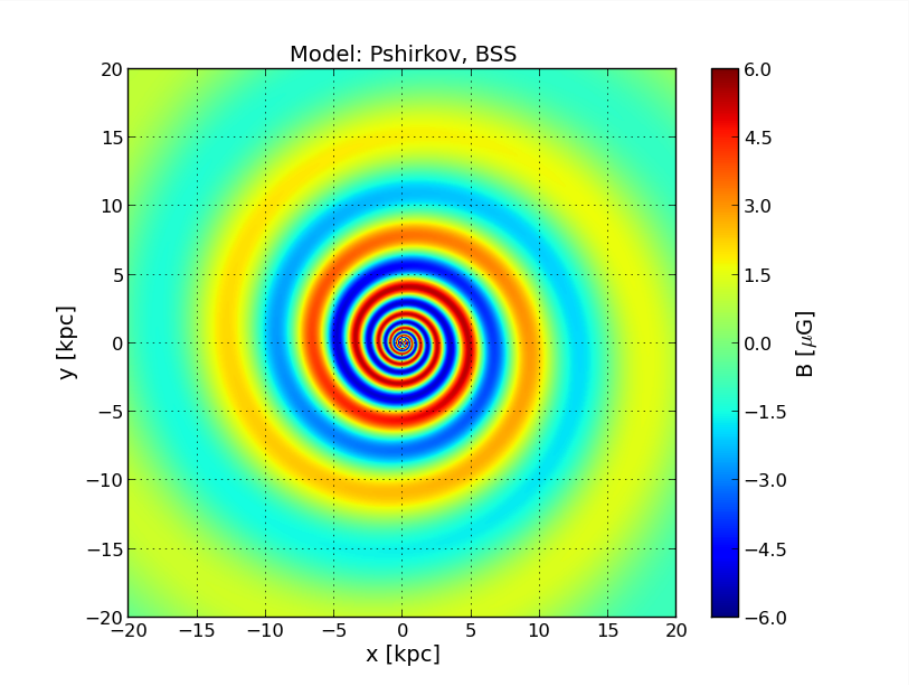

Figure 4: Bfield model: Pshirkov BSS model

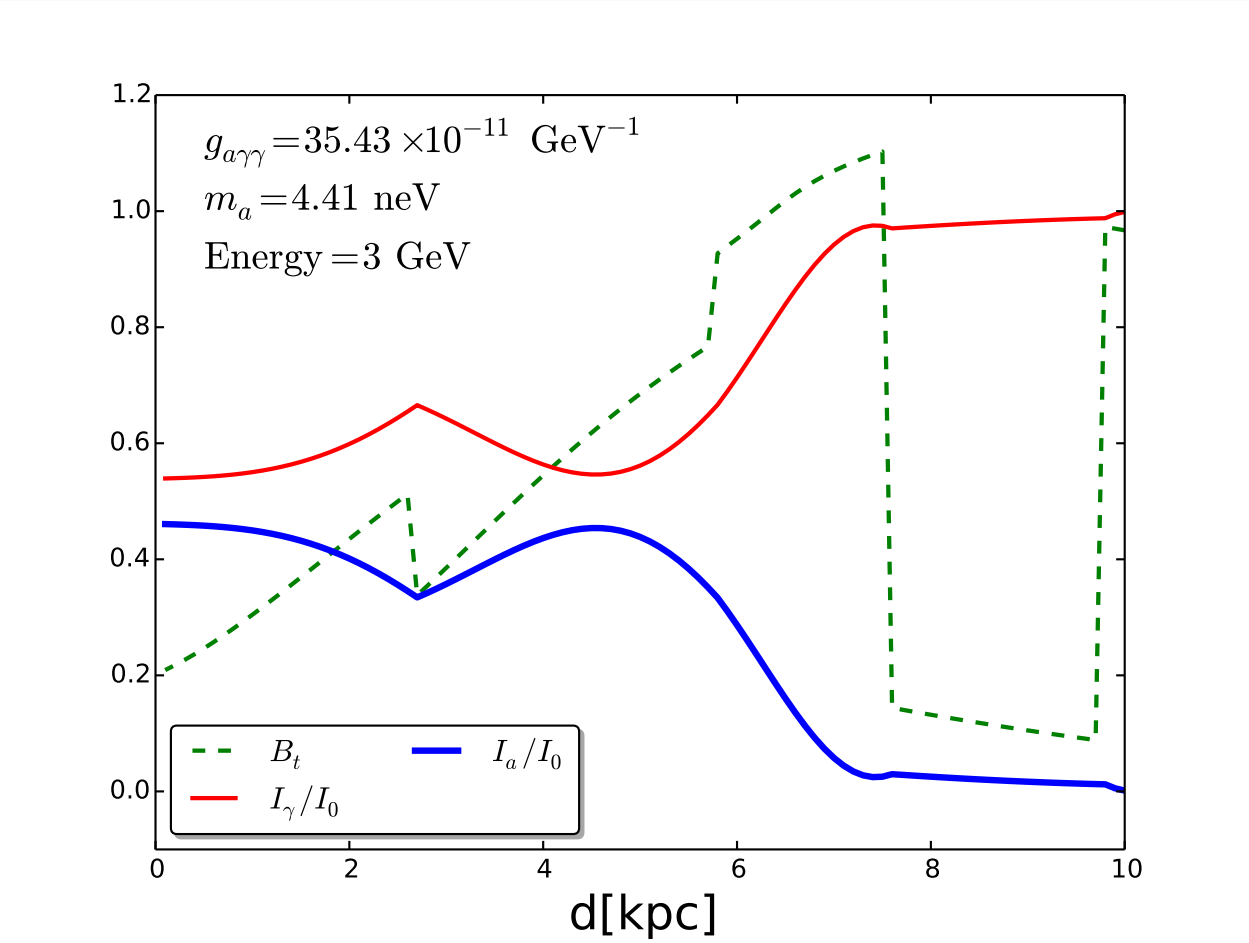

Photon (red thin line) and ALPs (blue thick line) intensity along the line of sight towards PSR J2021+3651. The green dashed line marks the transversal magnetic field.

Fermi-LAT data analysis

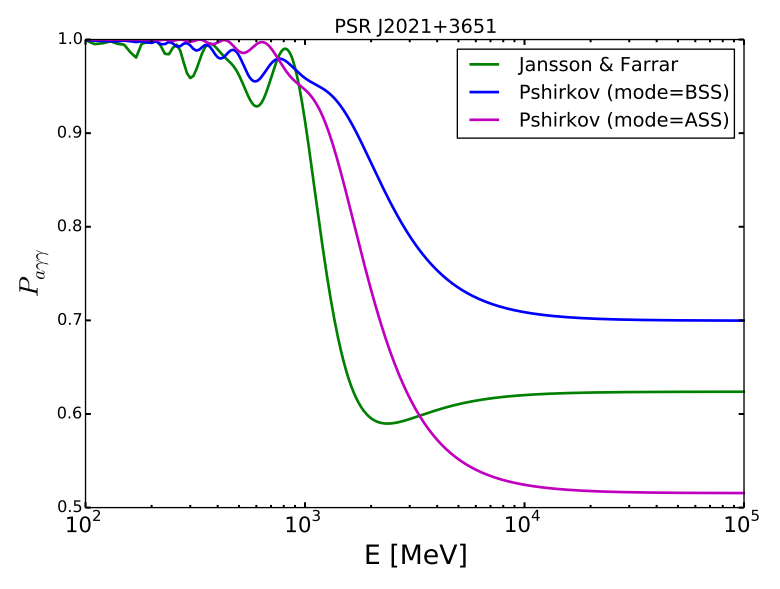

The photon survival probability as a function of energy.

$$\left(\frac{dN}{dE}\right)_{bin} = (1 - P_{\gamma \to a}\,(E, g_{a\gamma}, m_a)).\left(\frac{dN}{dE}\right)_{model,bin} \quad (16)$$

- We perform a fit to the data, minimising the χ^2 function.
- Log(likelihood) has a parabolic pattern.
- Energy dispersion matrix derived for all the EDISP event types together.

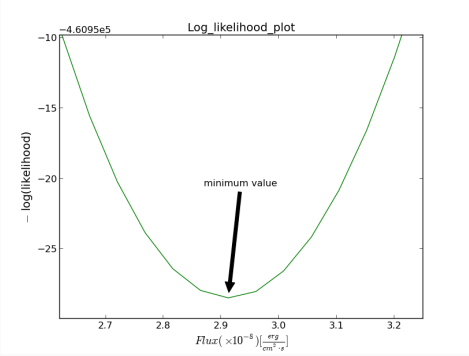

Log-likelihood as a function of flux for sixth energy bin of PSR J2021+3651.

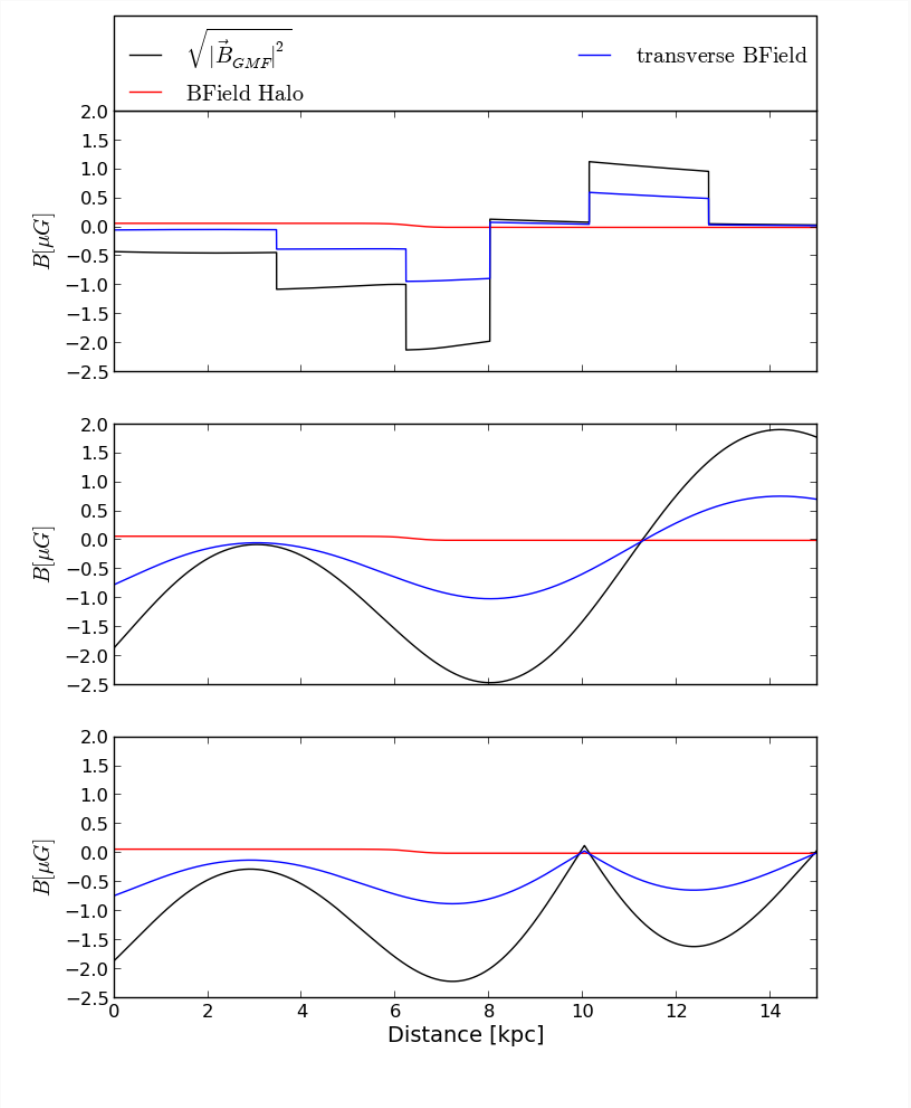

Figure 5: Bfield model:Magnetic field along the line of sight of the pulsar J2021 +3651.Top panel for the model of Jansson-Farrar, middle panel for the model of Pshirkov in BSS, bottom in ASS mode.

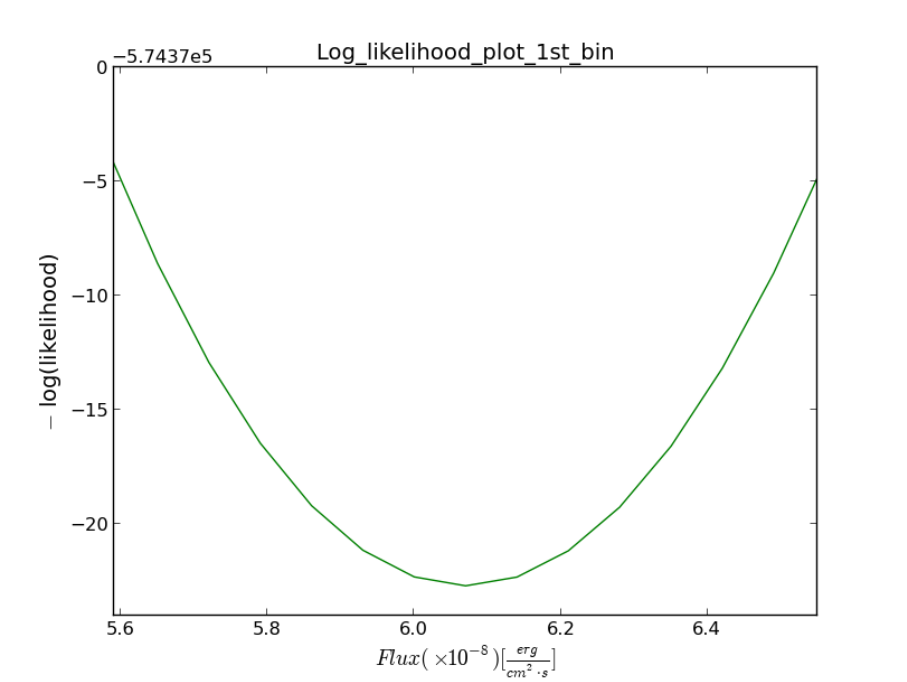

Figure 6: Log-likelihood as a function of flux for first energy bin of PSR J2021+3651.

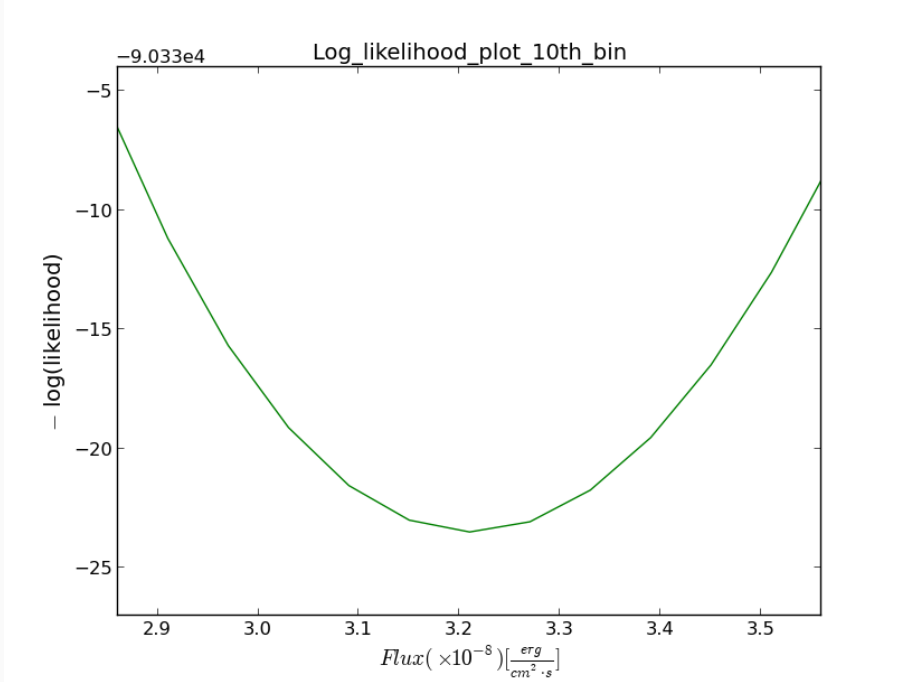

Figure 7: Log-likelihood as a function of flux for 10th energy bin of PSR J2021+3651.

Significance level

- Calculation of significance level: F-test is done.
- F-test: Test statistic has a F-distribution under the null hypothesis.
- F-test: statistical test to compare how well the model fits the population.
- F-number is constructed with :

$$f := \frac{(\chi^2_{\mathrm{H}_0} - \chi^2_{\mathrm{H}_1})/(m-k)}{\chi^2_{\mathrm{H}_1}/(n-m)} \sim F_{m-k,n-m}. \tag{17}$$

n= sample size,
m= no of parameters with ALPs
hypothesis,
k= no of parameters with no ALPs
hypothesis.

Contour dependence on magnetic field parameters and the distance to the source

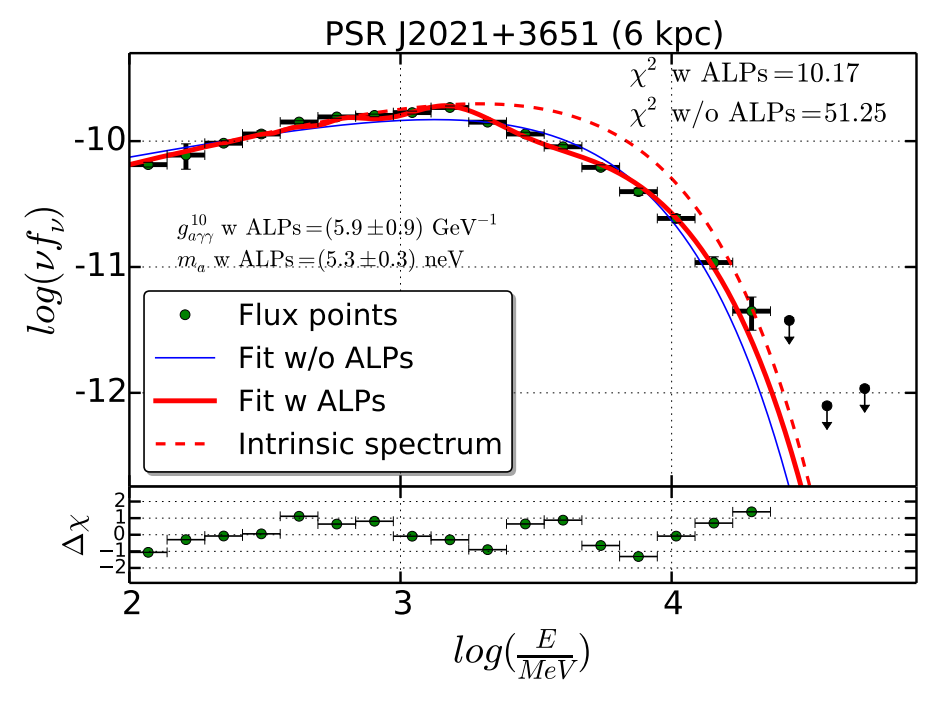

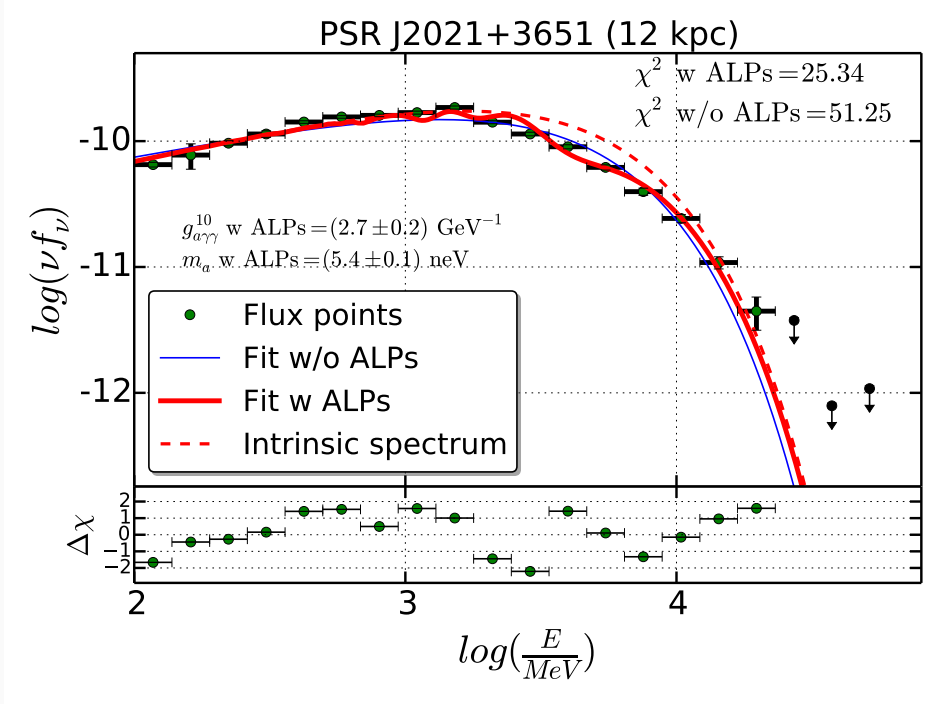

Reducing the distance by 4 kpc, we obtain a change $\approx 2.4 \times 10^{-10}\,\mathrm{GeV}^{-1}$, corresponding to around 70% enhancement in $g_{a\gamma\gamma}$.

When increasing the distance by 2 kpc, instead, $g_{a\gamma\gamma}$ changes by 24% and the mass varies around 1 neV.

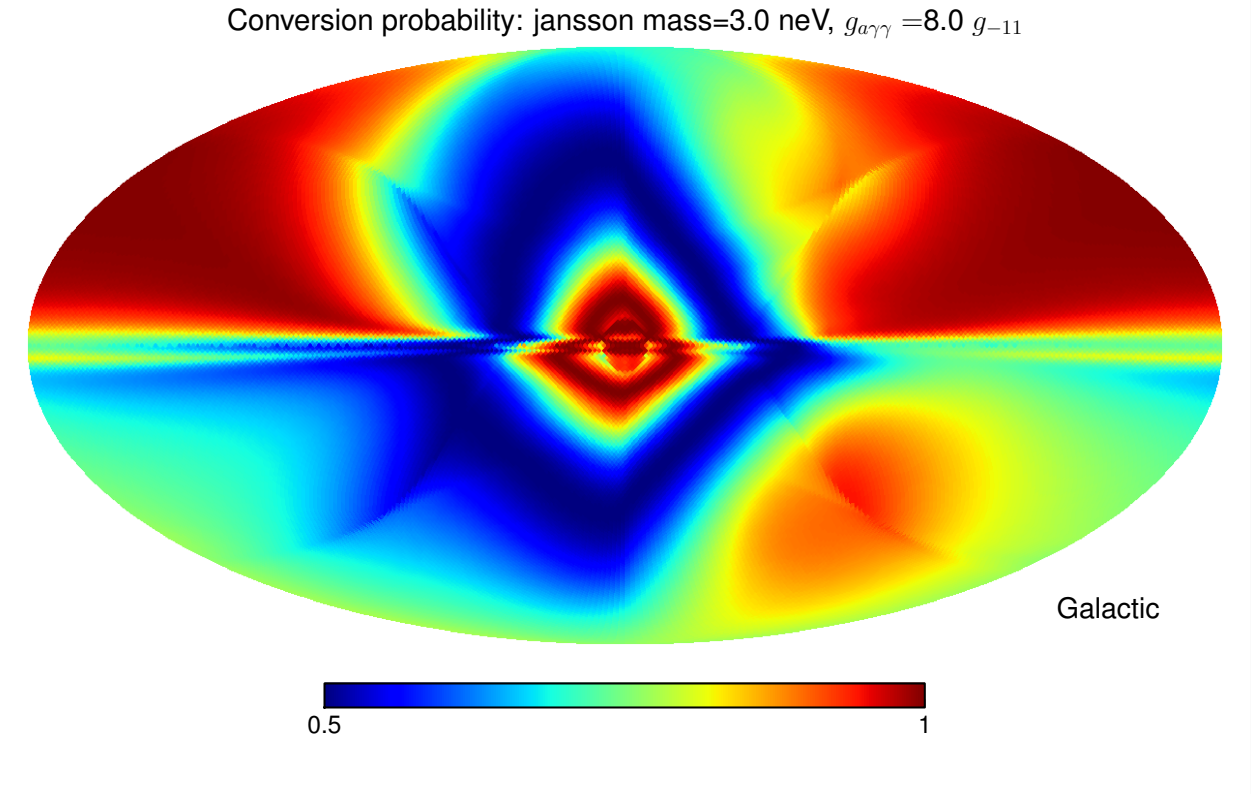

Figure 8: Conversion probability of photon to axion in allsky map.

Contour dependence on magnetic field parameters and the distance to the source

The variation of ALPs parameters calculated assuming diffrent Bfield and different distance for the global analysis.

Global analysis	$g_{a\gamma\gamma}$ (in $\times 10^{-10}\mathrm{GeV}^{-1}$)	m_a (in neV)
Bfield increased by 20%	2.1(4)	3.7(3)
Bfield decreased by 20%	2.6(2)	3.4(3)
Distance increased by 1kpc	2.3(4)	3.7(3)
Distance reduced by 1kpc	2.6(3)	3.6(3)
Distance increased by 1kpc and Bfield 20% increased	1.9(3)	3.7(3)
Distance reduced by 1kpc and Bfield 20% decreased	2.7(4)	3.6(3)

- $(m_a) = (3.6^{+0.5_{\mathrm{stat.}}}_{-0.2_{\mathrm{stat.}}} \pm 0.2_{\mathrm{syst.}})$ neV.
- $(g_{a\gamma\gamma}) = (2.3^{+0.3_{\mathrm{stat.}}}_{-0.4_{\mathrm{stat.}}} \pm 0.4_{\mathrm{syst.}}) \times 10^{-10}$ GeV^{-1}.